



## Limit State Equations for Stability and Deformation

Ibsen, Lars Bo; Jakobsen, K. P.

*Publication date:*  
1998

*Document Version*  
Publisher's PDF, also known as Version of record

[Link to publication from Aalborg University](#)

*Citation for published version (APA):*  
Ibsen, L. B., & Jakobsen, K. P. (1998). *Limit State Equations for Stability and Deformation*. Geotechnical Engineering Group. AAU Geotechnical Engineering Papers: Soil Mechanics Paper Vol. R 9828 No. 28

### General rights

Copyright and moral rights for the publications made accessible in the public portal are retained by the authors and/or other copyright owners and it is a condition of accessing publications that users recognise and abide by the legal requirements associated with these rights.

- Users may download and print one copy of any publication from the public portal for the purpose of private study or research.
- You may not further distribute the material or use it for any profit-making activity or commercial gain
- You may freely distribute the URL identifying the publication in the public portal -

### Take down policy

If you believe that this document breaches copyright please contact us at [vbn@aub.aau.dk](mailto:vbn@aub.aau.dk) providing details, and we will remove access to the work immediately and investigate your claim.

# **Limit State Equations for Stability and Deformation**

**L.B. Ibsen, K.P. Jakobsen**

---

**1998**

**Soil Mechanics Paper No 28**



**GEOTECHNICAL ENGINEERING GROUP  
AALBORG UNIVERSITY DENMARK**

**Ibsen, L.B., Jakobsen, K.P. (1998). Limit State Equations for Stability and Deformation.**

*AAU Geotechnical Engineering Papers*, ISSN 1398-6465 R9828.

*Soil Mechanics Paper No 28*

The paper has been published in

© 1998 AAU Geotechnical Engineering Group.

Except for fair copying, no part of this publication may be reproduced, stored in a retrieval system, or transmitted, in any form or by any means electronic, mechanical, photocopying, recording or otherwise, without the prior written permission of the Geotechnical Engineering Group.

Papers or other contributions in AAU Geotechnical Engineering Papers and the statements made or opinions expressed therein are published on the understanding that the author of the contribution is solely responsible for the opinions expressed in it and that its publication does not necessarily imply that such statements or opinions are or reflect the views of the AAU Geotechnical Engineering Group.

The AAU Geotechnical Engineering Papers - AGEP - are issued for early dissemination and book keeping of research results from the Geotechnical Engineering Group at Aalborg University (Department of Civil Engineering). Moreover, the papers accommodate proliferation and documentation of field and laboratory test series not directly suited for publication in journals or proceedings.

The papers are numbered ISSN 1398-6465 R<two digit year code><two digit consecutive number>. For internal purposes the papers are, further, submitted with coloured covers in the following series:

Series	Colour
Laboratory testing papers	sand
Field testing papers	grey
Manuals & guides	red
Soil Mechanics papers	blue
Foundation Engineering papers	green
Engineering Geology papers	yellow
Environmental Engineering papers	brown

In general the AGEP papers are submitted to journals, conferences or scientific meetings and hence, whenever possible, reference should be given to the final publication (journal, proceeding etc.) and not to the AGEPPaper.

## FINAL REPORT - VOLUME II - b CHAPTER 6

### 6 LIMIT STATE EQUATIONS FOR STABILITY AND DEFORMATION

L.B. IBSEN<sup>1)</sup> & K.P. JAKOBSEN<sup>2)</sup>

- 1) Associate Professor, University of Aalborg, Sohngaardsholmsvej 57, 9000 Aalborg, Denmark,  
e-mail: i5lbi@civil.auc.dk
- 2) Research Engineer, University of Aalborg, Sohngaardsholmsvej 57, 9000 Aalborg, Denmark,  
e-mail: i5kpj@civil.auc.dk

#### 6.1 Introduction

The soil beneath vertical breakwaters is subjected to a combination of forces induced by the waves. These forces can be characterised as (1) static load due to the submerged weight of the structure, (2) quasi-static forces induced by cyclic wave loading, and (3) wave impact from breaking waves on the vertical wall. A detailed explanation of the wave induced force is given in volume II a "Hydraulic Aspects". This chapter describes numerous geotechnical failure modes and corresponding limit state equations for monotonic, and dynamic loading of caisson breakwaters. The limit state equations presented herein are all estimated using the upper bound theory of classical plasticity theory. This approach, to formulate the limit state equations, is suitable for implementation in computational reliability programs.

The behaviour of granular materials can normally be accurately characterised by results from drained tests, since the materials can be considered fully drained in many practical problems. However, if the rate of loading is very high, such as that resulting from impact forces from breaking waves on vertical breakwaters, then essentially undrained conditions can exist. In addition, if the dimension of the breakwater is large and the permeability of the cohesionless soil is relatively low, significant pore-pressure changes may develop as a result of the quasi-static forces induced by cyclic wave loading, as described in Chapters 4 and 5. It will be explained how the limit state equations can be used for (1) quasi-static forces induced by cyclic wave loading, (2) wave impact from breaking waves on the vertical wall.

#### 6.2 General

In the following different failure modes for caisson breakwaters and the corresponding limit state equations will be presented. The failure modes have to be both statically and kinematically admissible. It is, however, difficult to find solutions that fulfil both conditions.



In practice this problem is solved by introducing different calculation tools in the design of large foundation structures, (Sørensen et al. 1993).

Normally the following calculation tools are used:

- Upper Bound Theory
- Limit Equilibrium Analysis
- Finite Element Analysis

Bearing capacities calculated by the Upper Bound Theory will be on the unsafe side of the correct solution compared to the Limit Equilibrium and the Finite Element Analysis. Normally the range between the three methods is very small.

### 6.2.1 Assumptions and Simplifications

The elaborated limit state equations can be used for pure frictional or cohesive materials. The contribution to the bearing capacity from cohesive layers is therefore expressed by the undrained shear strength  $c_u$  whereas the contribution from layers consisting of friction materials is due to its dilative behaviour,  $\psi$ , and the gravity  $\gamma'$  of the displaced soil mass. In traditional bearing capacity analysis this fundamental description of soils corresponds to an expectation of drained and undrained failure in the soil under static loading. When dealing with time varying loads it is, however, necessary to consider the possibility of instantaneous pore pressure build up during repetitive loading (see Section 4.1). For soils with low permeability the undrained condition and generation of pore pressure are evident, whereas for more permeable soils the possibility of undrained or partly undrained behaviour must be evaluated. This possibility of pore pressure build-up can be expressed in terms of the characteristic drainage period  $T_{ES}$  and the period of the wave load (see Section 4.2). The terms drained and undrained subsoil are adopted throughout the presentation of the limit state equations and it is up to the user to evaluate the actual drainage conditions.

A basic principle of the upper bound theory is the assumption of associated flow in the soil during shear. This prerequisite is fulfilled during undrained failure but is indubitably violated during drained failure, as the friction and dilation angle for frictional materials are quite different. This discrepancy is taken into account by use of a reduced effective friction angle  $\varphi_d$ , see Hansen (1979):

$$\tan \varphi_d = \frac{\sin \varphi' \cos \psi}{1 - \sin \varphi' \sin \psi} \quad (1)$$

## 6.2.2 Foundation Loads

The foundation loads are due to the net weight of the caisson, wave generated horizontal force on the caisson and seepage forces in the rubble mound. The wave generated horizontal force,  $F_H$ , is estimated using the formulas given in Volume II a "Hydraulic Aspects". The wave generated seepage forces, is as mentioned in Chapter 4, rather complicated to describe. It is for simplicity assumed that the seepage forces in the rubble mound can be described by one or two vertical components acting on impermeable horizontal boundaries and a horizontal component acting on the rupture boundary. As illustrated in Figure 1 has a simple linear approach been adopted for determination of the forces. As illustrated in the figure will the horizontal force on the rupture boundary and the downward force on the interface between rubble mound and subsoil depend on the height of the rubble mound and failure mode.

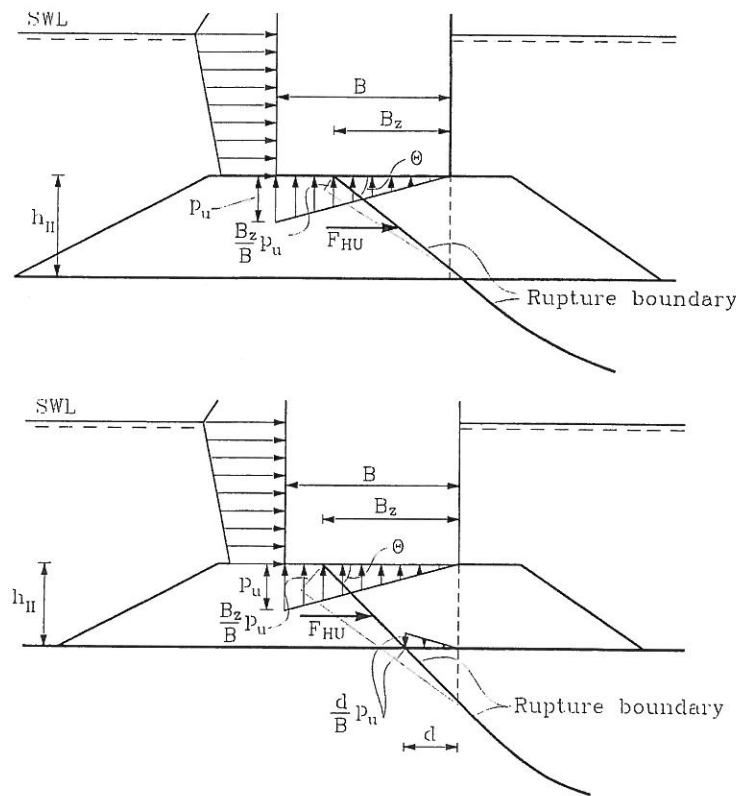


Fig. 1. Wave induced seepage forces.

The bottom of the caisson forms an impermeable horizontal boundary and is therefore subjected to a seepage generated vertical uplift. The determination of the vertical uplift,  $F_U$ , is discussed in Chapter 4 and given by equation 2.

$$F_U = \frac{B}{2} p_u \quad (2)$$

where

$B$  is the width of the caisson.

$p_u$  is the uplift pressure at the edge of the caisson.

The horizontal seepage force acting on the rupture boundary is rather complicated to determine as the variation of the pressure along the rupture boundary depends on several mechanical and geometrical quantities. The horizontal seepage force,  $F_{HU}$ , is for simplicity derived from equation 4, which is based on the approximated model illustrated in Figure 1.

$$F_{HU} = \begin{cases} \frac{B_z^2 - d^2}{2B} p_u \tan \theta & d > 0 \\ \frac{B_z^2}{2B} p_u \tan \theta & d \leq 0 \end{cases} \quad (4)$$

where

- $B_z$  is the effective width of the caisson.
- $d$  is the horizontal distance from the rear edge of the caisson to the point where the failure progresses into the subsoil.
- $\theta$  is the angle between the bottom of the caisson and the rupture boundary.

In cases where failure progresses into an undrained or impermeable subsoil can the seepage pressure generate a driving force on the interface between the rubble mound and subsoil. The force is for simplicity assumed to have the same distribution and magnitude as the uplift pressure. The downward pressure only affects the part of the subsoil that is included in the failure. Based on the principles outlined in Figure 1 it is possible to express the downward force,  $F_D$ , as in equation 3.

$$F_D = \begin{cases} \frac{d^2}{2B} p_u & d > 0 \\ 0 & d \leq 0 \end{cases} \quad (3)$$

From the figure and formulas above it is noticed that the principle of effective foundation width is adopted for derivation of the limit state functions and determination of seepage forces. This principle is known to be conservative, but it leads to limit state equations that are more applicable to engineering practice.

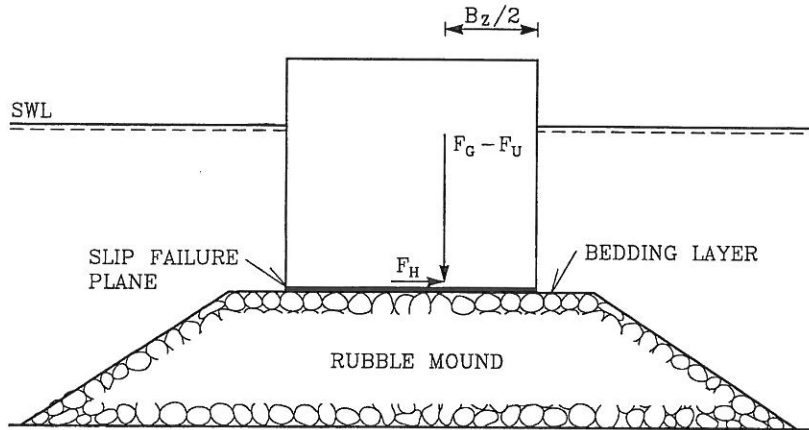
### 6.3 Limit State Equations

The limit state equations are obtained from three different groups of failure modes expresses the relation between external forces, geometric quantities and soil properties.

For the majority of the equations an optimisation on the geometric quantities is required for determination of the critical loads or bearing capacity. Optimisation parameters and constraints are given in these cases. Furthermore, a description of the mode of operation for each limit state equation is given. As the derived limit state equations are very voluminous only the principles of the limit state equations are stated. A thorough derivation of the limit state equations is found in Annex A.

## 6.3.1 Failure Mode: Sliding Over Foundation

Limit state equation 1

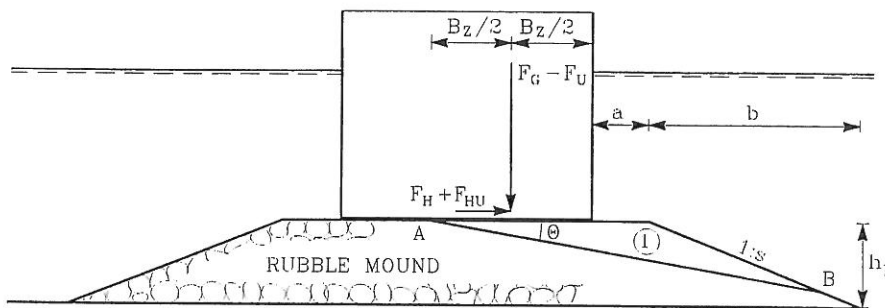
**Fig. 2.** Sliding between caisson and rubble mound.

The failure progresses as a horizontal displacement of the caisson due to lack of frictional resistance between the caisson and the bedding layer/rubble mound. The limit state equation, which is identical to Coulombs frictional hypothesis, is given in equation 3.

$$g = (F_G - F_U)\omega_{1V} - F_H\omega_{1H} = 0 \quad (5)$$

## 6.3.1 Failure Mode: Bearing Capacity Failure in Rubble Mound

Limit state equation 2

**Fig. 3.** Sliding through rubble mound.

Failure occurs as a simple rupture line from the bottom of the caisson and through the rubble mound. The failure is described by the optimisation parameter  $\theta$ . As the resistance against failure solely depends on the work from the displaced rubble mound material, the angle  $\theta$  must be within the limits given in 6. It is hereby ensured that a positive work contribution is

produced and that the failure lies within the rubble mound. The derived limit state equation is given in 7, where  $\omega_{1V}$ ,  $\omega_{1H}$  are the vertical and horizontal displacement of the soil mass in region 1.  $W_1$  is the work due to the gravity of displaced soil mass in region 1, see Annex A.

$$0 \leq \theta \leq \min\left(\varphi_{d1}; \tan^{-1}\left(\frac{h_{II}}{B_z + a + b}\right)\right) \quad (6)$$

$$g = W_1 + (F_G - F_U)\omega_{1V} - (F_H + F_{HU})\omega_{1H} = 0 \quad (7)$$

Limit state equation 3

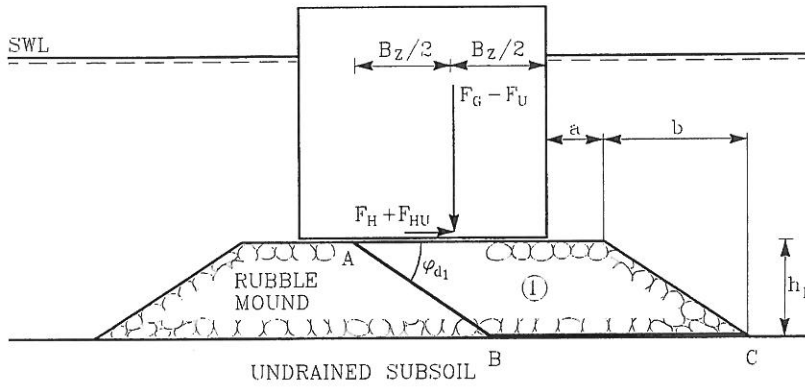


**Fig. 4:** Sliding in the transition zone between rubble mound and undrained subsoil.

Failure occurs as sliding in the transition zone between the rubble mound and undrained subsoil. As the caisson and region 1 are subjected to a horizontal displacement the resistance against failure is solely due to the shear resistance of the undrained subsoil along the rupture line  $l_{BC}$ . The angle between the bottom of the caisson and failure line through the rubble mound is given by the friction angle of the rubble mound material. The limit state equation is given in 8.

$$g = W_1 - (F_H + F_{HU})\omega_{1H} = 0 \quad (8)$$

Limit state equation 4

The failure occurs as a combination of line and zone failure in the rubble mound. Region 1 and 3 are displaced as rigid bodies, whereas region 2 consists of a zone failure rotating about point D. The limit state function is given in 9.

$$g = \sum_{i=1}^3 W_i + (F_G - F_U)\omega_{1V} - (F_H + F_{HU})\omega_{1H} = 0 \quad (9)$$

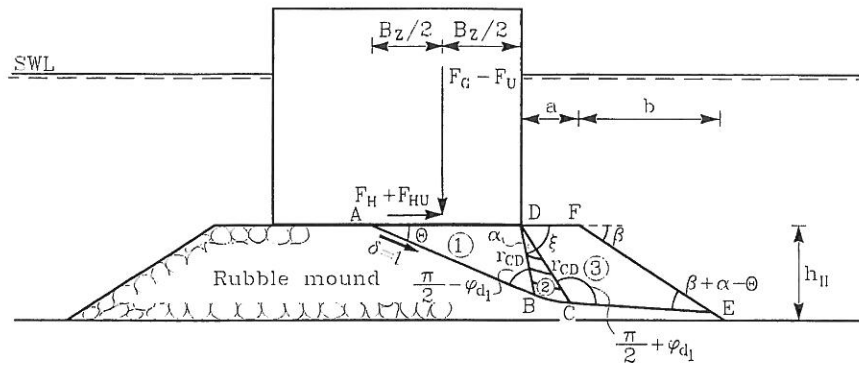


**Fig. 5.** Line and zone failure in rubble mound.

The geometry of the failure is controlled by the 2 free parameter's  $\theta$  and  $\alpha$  used for optimisation of the mechanism. To ensure that the failure will progress within the rubble mound the constraints given in 10-13 must be imposed.

$$\theta \geq 0 \quad (10)$$

$$0 \leq a \leq \theta \quad (11)$$

$$\beta + \alpha - \theta > 0 \quad (12)$$

$$A_3 \geq 0 \quad (13)$$

Limit state equation 5 (Constant volume)

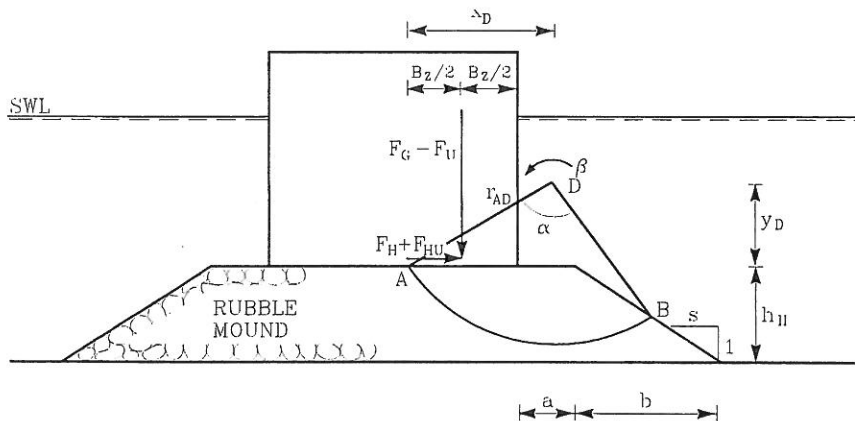


**Fig. 6.** Failure in rubble mound.

Limit state equation 5 is based on an assumption of constant volume conditions in the rubble mound. The limit state equation is therefore only valid if the failure load is reached within a short period of time. Under these circumstances the failure can be described by a single

circular slip line from the bottom of the caisson to a point located on the surface of the rubble mound. The resistance against failure is obtained from the shear resistance along the circular arc from A to B. In cases where point B is located on the inclined part of the rubble mound the displaced soil mass will affect the bearing capacity due to asymmetry and actually precipitate the failure. The limit state function is given in 14

$$g = \sum_{i=1}^3 W_i - (F_G - F_U) \left( x_D - \frac{B_z}{2} \right) \beta - (F_H + F_{HU}) y_D \beta = 0 \quad (14)$$

The limit state equation must be optimised with respect to the centre of rotation  $(x_D, y_D)$ . The constraints given in 15-17 must be imposed.

$$y_D \geq 0 \quad (15)$$

$$\frac{B_z}{2} \leq x_D \leq B_z + a + b \quad (16)$$

$$c \leq h_{II} \quad (17)$$

### 6.3.1 Failure Mode: Bearing Capacity Failure in Subsoil

Limit state equation 6

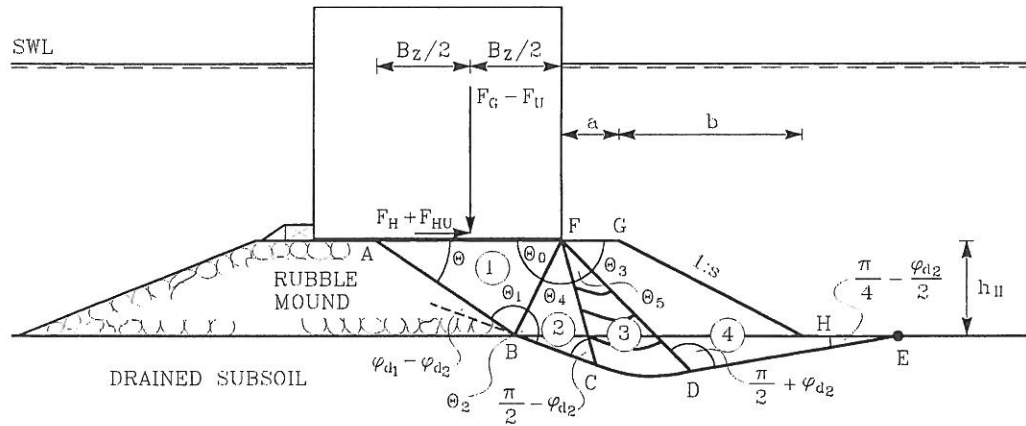


**Fig. 7.** Failure in rubble mound and drained subsoil.

Assuming that the rubble mound material has a higher strength than the drained subsoil and that the angle between the failure lines  $l_{AB}$  and  $l_{BC}$  correspond to the difference between the friction angles of the two materials, regions 1 and 2 will be displaced as one rigid body. Region 3 consists of a rupture zone rotating about point F. As the zone failure takes place in both the rubble mound and drained subsoil, the development of the zone is described by the weaker subsoil. Region 4 brings the rupture to the free surface of the subsoil by a rigid body



displacement. For regions 2 to 4 a possible difference in gravity between rubble mound and subsoil material is taken into account. The limit state function is given in 18.

$$g = \sum_{i=1}^4 W_i + (F_G - F_U)\omega_{1V} - (F_H + F_{HU})\omega_{1H} = 0 \quad (18)$$

The geometry of the failure is controlled by the free parameter  $\theta$  used for optimisation of the mechanism. To ensure that the failure will progress within the rubble mound the constraints given in 19-20 must be imposed.

$$\theta \geq \tan^{-1} \left( \frac{h_{II}}{B_7 + a + b} \right) \quad (19)$$

$$\theta_1 \geq \frac{\pi}{2} - \varphi_{d_1} \quad (20)$$

Limit state equation 7

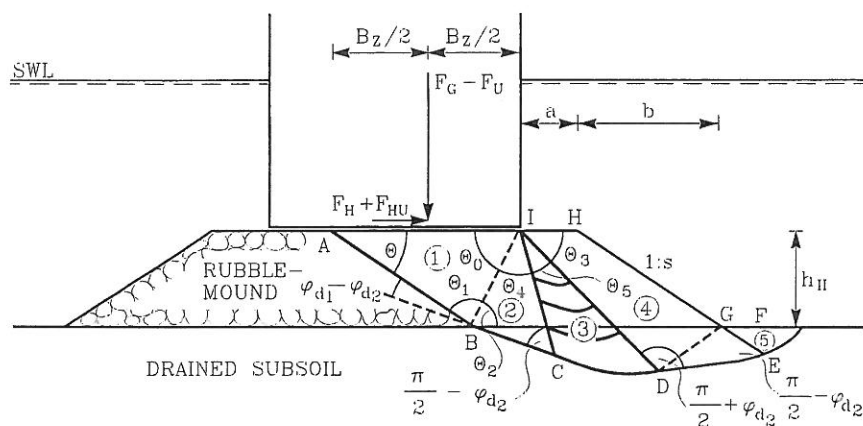


**Fig. 8.** Failure in rubble mound and drained subsoil.

Assuming that the rubble mound material has a higher strength than the drained subsoil and that the angle between the failure lines  $l_{AB}$  and  $l_{BC}$  corresponds to the difference between the friction angles of the two materials, regions 1 and 2 will be displaced as one rigid body. Region 3 consists of a rupture zone rotating about point F. As the zone failure takes place in both the rubble mound and drained subsoil, the development of the zone is described by the weaker subsoil. Region 5 brings the rupture to the free surface of the subsoil by a rupture zone rotating about the heel of the rubble mound (point G). Region 4, placed between the two rupture zones, moves as a rigid body. For regions 2 to 4 a possible difference in gravity between rubble mound and subsoil material is taken into account. The limit state equation is given in 21.





$$\theta \geq \max\left(0; \tan^{-1}\left(\frac{h_{II}}{B_z + a + b}\right) - \varphi_{d1}\right) \quad (24)$$

Limit state equation 9

The failure occurs as overturning of the breakwater. The failure consists of a logarithmic slip line in the rubble mound material and a circular slip line in the undrained subsoil. The mechanism is controlled by the centre of rotation and the corresponding distance to the heel of the rubble mound (point C). The resistance against failure is obtained from the gravity of the displaced soil in region 1 and the shear resistance along the circular arc from B to C.

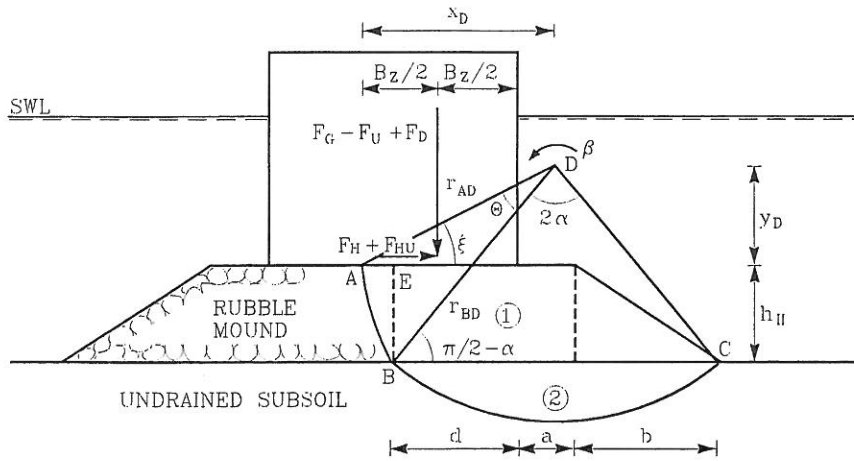


**Fig. 10.** Failure in rubble mound and undrained subsoil.

The derived limit state equation is given in 25, whereas the necessary constraints are given in 26-30.

$$g = \sum_{i=1}^2 W_i - (F_G - F_U + F_D) \left( x_D - \frac{B_z}{2} \right) \beta - (F_H + F_{HU}) y_D \beta = 0 \quad (25)$$

$$y_D \geq 0 \quad (26)$$

$$\frac{B_z}{2} \leq x_D \leq B_z + a + b \quad (27)$$

$$r_{BD} \cos \alpha = y_D + h_{II} \quad (28)$$

$$\alpha \geq 0 \quad (29)$$

$$\theta \geq 0 \quad (30)$$

## Limit state equation 10 (Constant volume)

Limit state equation 10 differs from limit state equation 9 in the description of the failure through the rubble mound. In the present case the failure is presumed to take place under constant volume conditions. For frictional materials this applies that failure loads must be reached within a short period of time, for example impact loading due to breaking waves. Under these circumstances the failure can be described by a single circular slip line from the bottom of the caisson to the heel of the rubble mound (point C).

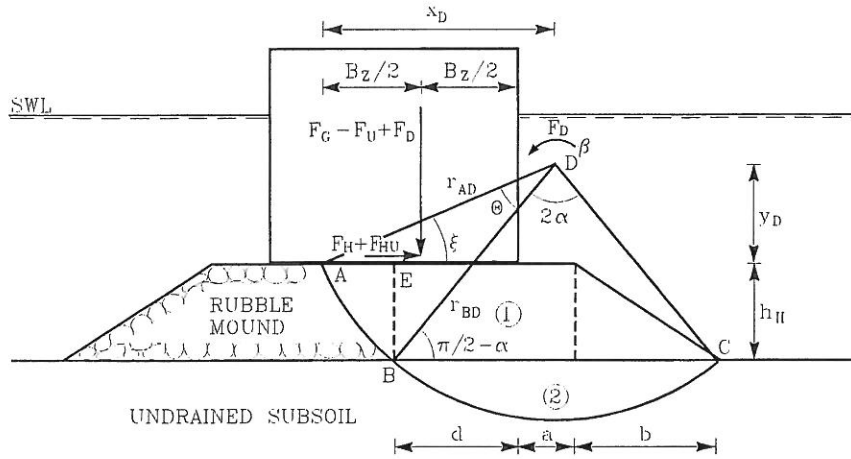


Fig. 11. Failure in rubble mound and undrained subsoil.

The resistance against failure is obtained from the gravity of the displaced soil in region 1 and the shear resistance along the circular arc from A to C. The derived limit state equation is given in 31, whereas the necessary constraints are identical to those given for limit state equation 9.

$$g = \sum_{i=1}^2 W_i - (F_G - F_U + F_D) \left( x_D - \frac{B_z}{2} \right) \beta - (F_H + F_{HU}) y_D \beta = 0 \quad (31)$$

#### 6.4 Influence of cyclic wave loading

As discussed in Chapter 5, the pore pressure increase depends on the intensity and duration of the cyclic load history and the drainage conditions, i.e. soil permeability, compressibility and drainage distance. If the drainage condition is limited a gradual accumulation of excess pore pressure may develop. This will cause a gradual reduction or increase of the effective stress in the soil. The influence of cyclic wave loading, i.e. the effect of “precycling” and accumulation of excess pore pressure, is taken into account by following the guidance given in Chapter 5. The shear strength depends on the effective stresses in the soil, and thus on the excess pore pressure generated during the storm. The shear strength is further dependent on whether the soil is contractive or dilative during the shearing under the extreme loads and whether this takes place under drained, partly drained or undrained conditions. If the breakwater is not exposed to impact wave loading the increased or reduced strength parameters, due to the influence of cyclic wave loading should be used.

The gravel and the rockfills of the mound will be drained and clay will be undrained during the period of one wave cycle. The stability of the breakwater is evaluated by using limit state equations 1, 2, 3, 4, 8 and 9.

Sand may be partly drained during the period of one wave cycle and it is necessary to consider whether the partial drained or the drained shear strength should be used in the stability calculations. The stability of the breakwater is evaluated by using limit state equations 1, 2, 4, 6 and 7. After soil is loaded close to failure and subsequently unloaded, a small permanent deformation remains. Significant permanent deformations remain if several cycles of extreme loading and subsequent unloading occur briefly after each other, so briefly that hardly any drainage takes place during the considered cycles. This phenomenon is usually referred to as “cyclic mobility”, and it results in cyclic residual deformations.

Cyclic mobility may result in unacceptable deformation of the foundation of a vertical breakwater on a subsoil of clay, silt or fine sand (characteristic drainage period  $T_{ES}$  larger than approximately 10 times the wave period, see Section 4.2). In design of breakwaters the cyclic residual deformations need to be restricted to an allowable measure. This means that the cyclic stress amplitude has to be limited to such a value that within the expected number of wave loads a certain residual shear strain is not exceeded. The Database (NGI, 1999) contains diagrams that give the cyclic shear strain relative to the average shear stress and shear stress amplitude. Some diagrams are presented in chapter 2 of this volume.

The analysis to restrict cyclic residual strain requires the following steps:

- Select the maximum acceptable residual shear strain
- Perform a sliding plane analysis with the load induced by the weight load and the average between extreme wave load (at wave crest) and the minimum wave load (at wave trough) to calculate the average shear load along potential sliding planes.
- Derive the acceptable cyclic shear amplitude for all parts of each potential sliding plane from the Database graphs, with respect to the selected maximum acceptable residual shear strain.
- Perform sliding plane analysis with the extreme wave load, find the resulting shear stress and compare it with the allowable.

A complete description of the required steps can be found in Andersen and Lauritzen (1988).

## 6.5 Influence of impact wave loading

In practice undrained failure in frictional materials is of rare occurrence. This failure state must, however, be considered in a design situation where there is a possibility for impact wave loading. Whether drained or undrained failure occurs depends on the grain size distribution and void ratio of the material, but for fine frictional materials as sand undrained failure may actually occur during the short peak loads from wave impacts. The undrained shear strength of the frictional material should under these circumstances be evaluated as described below. For coarse materials as the gravel and rock fill of the mound the occurrence

of an undrained failure is questionable. It could instead be argued that the failure in these materials progresses under constant volume as the duration of the impact is so short that dilation hardly occurs. Under these conditions the shear strength of the gravel and rock fill should be used. Limit state equations 5 and 10 are especially derived for evaluation of constant volume and undrained failure.

### 6.5.1 Undrained shear strength of frictional materials

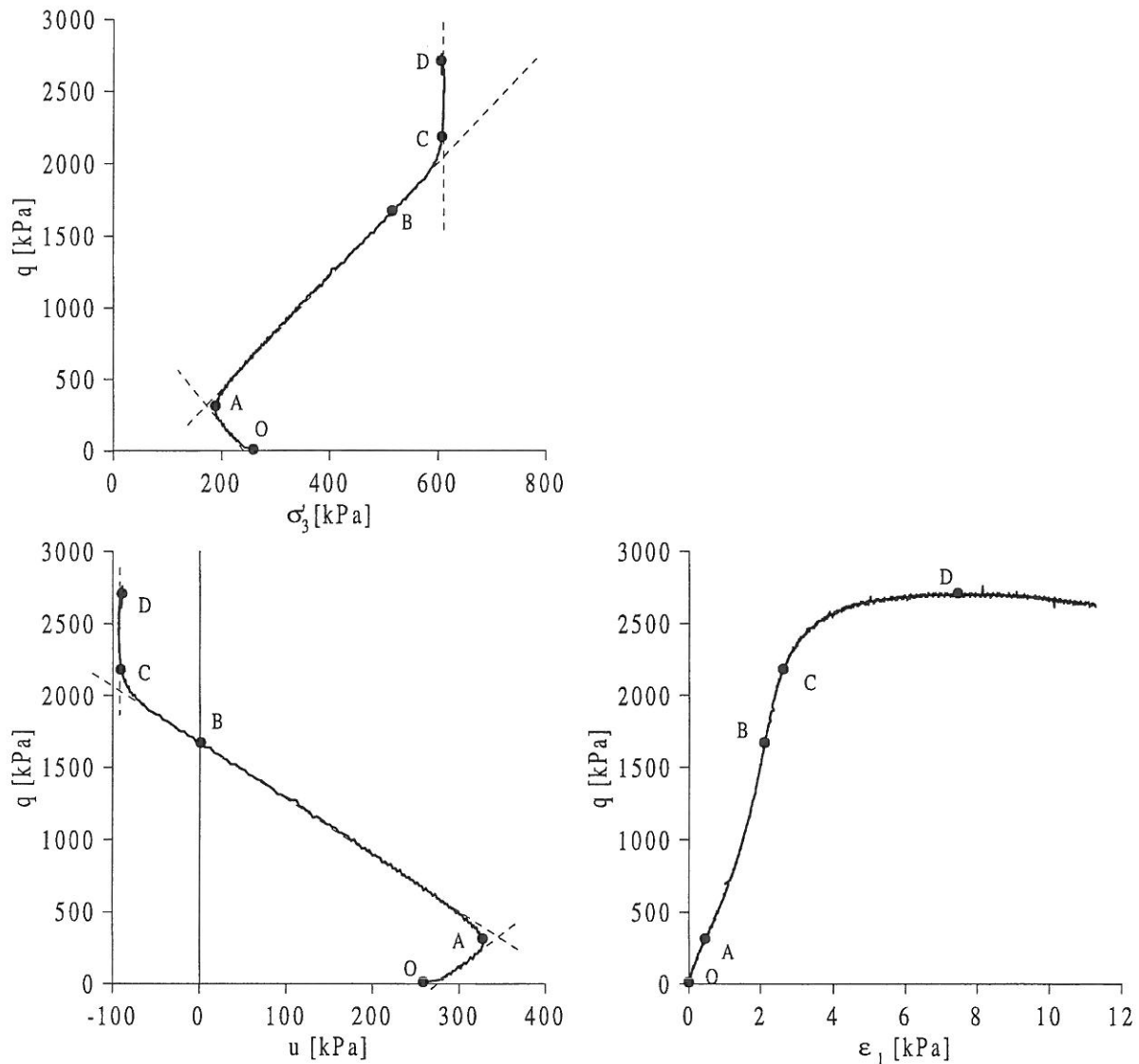


**Fig. 12.** Results of undrained triaxial test performed on Aalborg University Sand No. 1. The test was performed with a constant deformation rate of 100 % per hour. The specimen was prepared with  $e=0.55$  corresponding to  $D_R=100\%$ .

It is known from constant volume tests that the tendency to contraction or dilation of the soil skeleton is forcefully resisted by the pore fluid creating a positive or negative increase in the

pore pressure. In the majority of the cases the pore fluids resistance against volume changes will lead to a strengthening of the soil. The phenomenon static liquefaction only occurs for very loose deposits. An example of undrained soil response is given in Figure 12. The figure shows that the pore pressure initially increases to prevent the sand from contraction,  $\delta u > 0$ . When the effective stress state approaches the characteristic stress state (CS), point A,  $\delta u \rightarrow 0$ . Between point A and B the pore water manages to prevent the sand from dilating and the pore pressure generation is negative,  $\delta u < 0$ . Up to point B the effective stress path follows the common stress path (CSP) defined by the drained stress states where  $\Sigma \delta \epsilon_v = 0$ . When the pore pressure becomes negative the response changes character. The pore water can no longer fully prevent the dilation and the response starts to deviate from the common stress path. At point C the pore water provides the maximum resistance and cavitation occurs at approximately -90 to -100 kPa, corresponding to the atmospheric pressure. From this state the effective confining pressure remains constant, and further strengthening of the material depends entirely on the dilatation. At point D failure occurs, while the negative pore pressure remains constant and does not vanish between point C and D.

Based on the characteristics given above the undrained shear resistance for frictional materials can easily be determined at a given point beneath the structure. The determination requires knowledge of the effective friction angle, initial effective state of stress corrected for the influence of the cyclic loading ( $\sigma'_{3i}$ ,  $\tau_i$ ) and the maximum pore pressure that can be generated during shear. The maximum negative pore pressure that can be generated during shear equals the initial hydrostatic pressure  $u_h$  plus the atmospheric pressure  $p_a$ . The principle of the method is illustrated in Figure 13.

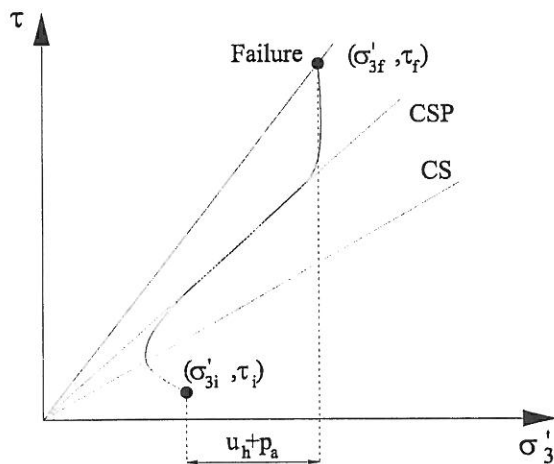


Fig. 12. Principle of the determination of the undrained shear strength.

The undrained shear strength of the frictional material is given by the following relation:

$$c_u = \tau_f = \sigma'_{3f} \frac{\sin \varphi'}{1 - \sin \varphi'} = (\sigma'_{3i} + u_h + p_a) \frac{\sin \varphi'}{1 - \sin \varphi'} \quad (32)$$

If the dilating sand and gravel are not fully saturated one should be careful about relying on the higher shear strength due to negative pore pressures.

## 6.6 Deformations due to impact wave loading

During extreme high wave impacts, the loading may exceed the static bearing capacity of the foundation for a short period. This exceeding will cause permanent deformations of the foundation, but due to inertia or dynamic strengthening of the soil the deformations may be small enough to be acceptable. The model presented in this section is developed for evaluation of such permanent deformations. The model is based on the upper bound theory of classical plasticity theory and settles with the classical elastic methods. This change of approach is necessary, as the elastic method is inadequate in cases where the impact load is so significant that it doubtless will cause permanent plastic deformations of the foundation.

Experience shows that the soil under impact loading normally will produce a reaction, which exceeds the static capacity. This additional capacity emanates from inertia forces, geometrical changes and an additional strengthening of the soil due to the dynamic loading. The model takes these contributions into account and allows for impact loading that exceeds the static bearing capacity.

The principle of the model is given in the succeeding sections and an example of the application is given in Annex B.

### 6.6.1 Principle of the Dynamic Model

As described above the dynamic model is based on the upper bound theory of classical plasticity theory. Example on the use of this theory was given in Section 6.3 for various failure modes and corresponding limit state equations for caisson breakwaters subjected to static or quasi-static loading.

The first step in the dynamic analysis includes a determination of the critical limit state equation under static loading. The knowledge gained from this analysis, e.g. bearing capacity, displacement field and geometrical quantities describing the failure, forms basis of the further investigation.

As the foundation is subjected to a dynamic impulse,  $I(t)$ , that exceeds the static bearing capacity,  $F$ , a failure state is reached and the structure and the subsoil will be accelerated and displaced. The deformation of the system will progress until the dynamic contributions at a given time counteract the dynamic impulse. As the model is based on the assumption of rigid



plasticity the deformation stops when the deformation velocity reaches zero and the permanent deformation is directly obtained.

### 6.6.2 Dynamic Impulse

The description of the dynamic impulse or dynamic load history is in general attended with great difficulties due to the highly stochastic processes involved. For impact wave loading the deficiency is mainly due to the large number of influencing parameters related to the geometry of the structure and foreshore, as well as the effect of entrapped air in breaking waves. Results, however, show that for waves breaking on the structure the load history contains one or two peaks followed by rapid decay to the quasi-static load level, Oumeraci and Kortenhaus (1995). These characteristics have lead to two simple descriptions of the impulse given in Figure 14.

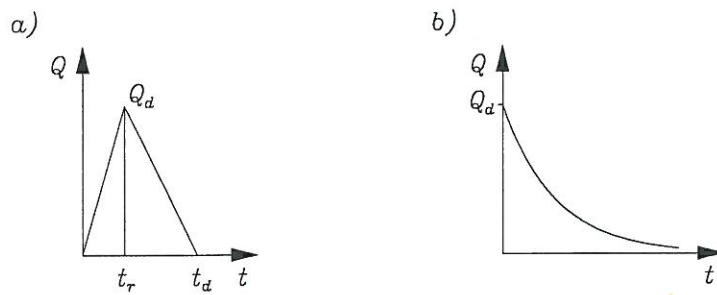


**Fig. 13.** a) Triangular load history, Oumeraci and Kortenhaus (1995). b) Exponential load history.

It may be argued that the descriptions are oversimplified, but with the difficulties attached to the characterisation of the impulse and the fact that the present dynamic model only accounts for loads that exceed the static bearing capacity of the foundation the procedures are found reasonable. The mathematical formulation for the two load histories is given in equation 33. The triangular load history is given by the peak force  $Q$ , the rise time  $t_r$  and the decay time  $t_d$ .

$$I(t) = \begin{cases} Q_d \frac{t}{t_r} & 0 \leq t < t_r \\ Q_d \left(1 - \frac{t - t_r}{t_d - t_r}\right) & t_r \leq t < t_d \\ 0 & t_d \leq t \end{cases} \quad (33)$$

In cases where the rise time is very short it is found convenient to describe the load history by a simple exponential function given by the peak force and a constant of decay  $k$ .

$$I(t) = Q_d e^{-kt} \quad (34)$$



For use with the dynamic model it is convenient to express the magnitude of the impact relative to the static bearing capacity by an overloading factor  $S$ :

$$S = \frac{Q_d}{F} \quad (35)$$

A more thorough description is found in Annex B.

### 6.6.3 Dynamic Contributions

The necessary information about displacements and accelerated masses is fully deduced from the static analysis in form of predefined displacement diagrams and geometrical quantities.

Inertia forces due to acceleration of the structure and the soil mass will, in accordance with Newton's 2 law, contribute to the system's resistance against deflection. The inertia of the system is found by summing up the inertia from structure and the different failure regions:

$$\Delta F^m(\ddot{w}) = \sum_{i=1}^{i=n} \ddot{w} A_i \rho_i \quad (36)$$

Whenever the bearing capacity is exceeded soil will be pushed up at the side of the foundation and increase the stabilising earth pressure. The displacement of the soil will, however, at the same time lead to a reduction of the shear resistance due to a shortening of the failure lines. This effect of geometrical changes can be expressed as:

$$\Delta F^k(\omega) = \gamma \Delta A(\omega) - \int_0^{\omega} c_u(s) ds \quad (37)$$

The effect of the geometrical changes will either lead to a strengthening of the foundation or precipitate failure. Thus the effect must be evaluated in each case.

Besides these contributions due to inertia and geometrical changes the displacement velocity might affect the strength of the soil. Several tests have been performed in order to investigate the effect of deformation rates on the strength of both cohesive and frictional soils. For frictional materials the strength seems to be independent of the displacement velocity (Ibsen, 1995), whereas the strength of cohesive soils is found to increase with increasing displacement velocity. This partially viscous behaviour is described by Bjerrum (1971) and by Kulhawy and Mayne (1990) and may be expressed as:

$$c_u^d(\dot{w}) = c_u + \kappa c_u \log \dot{w} \approx c_u + \Delta c_u^d \dot{w} \quad (38)$$

The effect on the failure mechanisms shear resistance can be formulated as in 39 by summing up contributions from the different failure lines and regions:

$$\Delta F^c(\dot{\omega}) = \int_L c_u^d(s, \dot{\omega}) - c_u(s) ds + \iint_A c_u^d(s, \dot{\omega}) - c_u(s) ds dl \quad (39)$$

#### 6.6.4 Equation of Motion

The dynamic terms given in 36, 37 and 39 together with the static bearing capacity and the dynamic impulse yield the equation of motion with one degree of freedom:

$$I(\ddot{t}) = F + \Delta F^m(\ddot{\omega}) + \Delta F^c(\dot{\omega}) + \Delta F^k(\omega) \quad (40)$$

The permanent deformation of the system can be determined by solving the equation of motion and following the principles outlined in Section 6.6.1. The solution to the equation of motion depends on the actual failure mode and the dynamic contributions. An example of the application of the model is given in Annex B.

### 6.7 References

- BJERRUM, L. (1971): Effect of Rate of Strain on Undrained Shear Strength of Soft Clay. *Norwegian Geotechnical Institute. Publ. 85*, pp. 41-42.
- HANSEN, B. (1979): Definition and use of frictional angles. *Proc. Int. Conf. VII ECSMFE*, Brighton, UK.
- IBSEN, L.B. (1995): The Static and Dynamic Strength of Sand. *Proc. Int. Conf. XI ECSMFE*, Copenhagen, DK.
- KULHAWY, F.H.; MAYNE, P.W. (1990): Manual on Estimating Soil Properties for Foundation Design. *Cornell University, Ithaca, New York*, pp. 4.48-4.49.
- OUMERACI, H.; KORTENHAUS, A. (1995): Note on Wave Loading for Foundation Design of Caisson Breakwaters. *Foundation Design of Caisson Breakwaters, MSC-Project, MAS2-CT92-0047, Vol. 2*, 18 pp.
- SØRENSEN, C.S.; CLAUSEN, C.J.F.; ANDERSEN, H. (1993): Bearing Capacity Analysis for the Great Belt East Bridge Anchor Blocks. *Limit State Design in Geotechnical Engineering, ISLSD 93*, pp. 305-312.
- ANDERSEN, K.H.; LAURITZSEN (1988): Bearing Capacity for Foundations with Cyclic Loads. *Journal of the Geotechnical Engineering Division, ASCE, Vol. 114, No. GT5*

### 6.8 Symbols

The list only includes the most common symbols. Additional quantities are explained in the text or will appear from the figures.

A	[m <sup>2</sup> ]:	Area
B	[m]:	Foundation width
B <sub>z</sub>	[m]:	Effective foundation width
c <sub>u</sub>	[kPa]:	Undrained shear strength

$F$	[kN/m]:	Force
$F_G$	[kN/m]:	Force due to gravity
$F_U$	[kN/m]:	Force due to upward seepage pressure
$F_D$	[kN/m]:	Force due to downward seepage pressure
$F_H$	[kN/m]:	Horizontal force
$F_{HU}$	[kN/m]:	Horizontal component of wave induced pressure
$H$	[m]:	Height of structure
$J$	[kgm]:	Mass moment of inertia
$M$	[kNm/m]:	Moment
$p_u$	[kPa]:	Upward pressure
$p_d$	[kPa]:	Downward pressure
$p_a$	[kPa]:	Atmospheric pressure
$Q_d$	[kN/m]:	Magnitude of dynamic pulse
$u$	[kPa]:	Pore pressure
$u_h$	[kPa]:	Hydrostatic pore pressure
$S$	[-]:	Dynamic overloading factor
$W$	[kNm/m]:	External and internal work
$x$	[m]:	Horizontal distance
$y$	[m]:	Vertical distance
$\delta$	[m]:	Unit displacement
$\beta$	[°]:	Angle of rotation
$\varphi$	[°]:	Friction angle
$\varphi_d$	[°]:	Reduced friction angle
$\psi$	[°]:	Angle of dilatation
$\gamma$	[kN/m <sup>3</sup> ]:	Specific weight
$\omega$	[m]:	Displacement
$\rho$	[kg/m <sup>3</sup> ]:	Density
$\sigma_3$	[kPa]:	Confining pressure, horizontal stress
$\tau$	[kPa]:	Shear stress, shear strength

### Subscripts

$i$	:	Summational parts, layer, initial state or region
$G$	:	Parameter relative to centre of rotation or centre of gravity
$f$	:	Failure
$H$	:	Horizontal
$V$	:	Vertical
$AB$	:	Paired subscripts in capital letters are used for the length between adjacent points (e.g. point A and B)

### Superscripts

$'$	:	Denotes effective parameter
$k$	:	Dynamic contribution due to geometric changes
$d$	:	Dynamic property (strengthening due to dynamic loading)
$m$	:	Dynamic contribution due to inertia

## AGEP: Environmental Engineering papers

- 12 Lade, P.V., Ibsen, L.B. (1997). A study of the phase transformation and the characteristic lines of sand behaviour. Proc. Int. Symp. on Deformation and Progressive Failure in Geomechanics, Nagoya, Oct. 1997, pp. 353-359. Also in *AAU Geotechnical Engineering Papers*, ISSN 1398-6465 R9702.
- 13 Bødker, L., Steenfelt, J.S. (1997). Vurdering af lodrette flytningsamplituder for maskinfundament, Color Print, Vadum (Evaluation of displacement amplitudes for printing machine foundation; in Danish). *AAU Geotechnical Engineering Papers*, ISSN 1398-6465 R9706.
- 14 Ibsen, L.B., Steenfelt, J.S. (1997). Vurdering af lodrette flytningsamplituder for maskinfundament Løkkensvejens kraftvarmeværk (Evaluation of displacement amplitudes for gas turbine machine foundation; in Danish). *AAU Geotechnical Engineering Papers*, ISSN 1398-6465 R9707.
- 15 Steenfelt, J.S. (1997). National R&D Report : Denmark. *Seminar on Soil Mechanics and Foundation Engineering R&D*, Delft 13-14 February 1997. pp 4. Also in *AAU Geotechnical Engineering Papers*, ISSN 1398-6465 R9708.
- 16 Lemonnier, P. and Soubra, A. H. (1997). Validation of the recent development of the displacement method - geogrid reinforced wall. *Colloquy EC97 on the comparison between experimental and numerical results*, Strasbourg, France. Vol.1, pp. 95-102. Also in *AAU Geotechnical Engineering Papers*, ISSN 1398-6465 R9712.
- 17 Lemonnier, P. & Soubra, A. H. (1997). Recent development of the displacement method for the design of geosynthetically reinforced slopes - Comparative case study. *Colloquy on geosynthetics, Rencontres97, CFG*, Reims, France, Vol. 2, pp. 28AF-31AF (10pp). Also in *AAU Geotechnical Engineering Papers*, ISSN 1398-6465 R9713.
- 18 Lemonnier, P., Soubra, A. H. & Kastner, R. (1997). Variational displacement method for geosynthetically reinforced slope stability analysis : I. Local stability. *Geotextiles and Geomembranes* 16 (1998) pp 1-25. Also in *AAU Geotechnical Engineering Papers*, ISSN 1398-6465 R9714.
- 19 Lemonnier, P., Soubra, A. H. & Kastner, R. (1997). Variational displacement method for geosynthetically reinforced slope stability analysis : II. Global stability. *Geotextiles and Geomembranes* 16 (1998) pp 27-44. Also in *AAU Geotechnical Engineering Papers*, ISSN 1398-6465 R9715.
- 20 Ibsen, L.B. (1998). Analysis of Horizontal Bearing Capacity of Caisson Breakwater. 2nd PROVERS Workshop, Napels, Italy, Feb. 24-27-98. Also in *AAU Geotechnical Engineering Papers*, ISSN 1398-6465 R9802.
- 21 Ibsen, L.B. (1998). Advanced Numerical Analysis of Caisson Breakwater. 2nd PROVERS Workshop, Napels, Italy, Feb. 24-27-98. Also in *AAU Geotechnical Engineering Papers*, ISSN 1398-6465 R9803.
- 22 Ibsen, L.B., Lade P.V. (1998). The Role of the Characteristic Line in Static Soil Behavior. *Proc. 4th International Workshop on Localization and Bifurcation Theory for Soil and Rocks*. Gifu, Japan. Balkema 1998. Also in *AAU Geotechnical Engineering Papers*, ISSN 1398-6465 R9804.



## AGEP: Environmental Engineering papers

- 23 Ibsen, L.B., Lade, P.V. (1998). The Strength and Deformation Characteristics of Sand Beneath Vertical Breakwaters Subjected to Wave Loading. 2nd PROVERS Workshop, Napels, Italy, Feb. 24-27-98. Also in *AAU Geotechnical Engineering Papers*, ISSN 1398-6465 R9805.
- 24 Steenfelt, J.S., Ibsen, L.B. (1998). The geodynamic approach - problem or possibility? Key Note Lecture, *Proc. Nordic Geotechnical Meeting, NGM-96, Reykjavik, Vol 2*, pp 14. Also in *AAU Geotechnical Engineering Papers*, ISSN 1398-6465 R9809.
- 25 Lemonnier, P., Gotteland, Ph. and Soubra, A. H. (1998). Recent developments of the displacement method. *Proc. 6th Int. Conf. on Geosynthetics. Atlanta, USA, Vol 2*, pp 507-510. Also in *AAU Geotechnical Engineering Papers*, ISSN 1398-6465 R9814.
- 26 Praastrup, U., Jakobsen, K.P., Ibsen, L.B. (1998). On the choice of strain measures in geomechanics. 12<sup>th</sup> Young Geotechnical Engineers Conference, Tallin, Estonia. *AAU Geotechnical Engineering Papers*, ISSN 1398-6465 R9815.
- 27 Ibsen, L.B. (1998). The mechanism controlling static liquefaction and cyclic strength of sand. *Proc. Int. Workshop on Physics and Mechanics of Soil Liquefaction, Baltimore. A.A.Balkema, ISBN 9058090388*, pp 29-39. Also in *AAU Geotechnical Engineering Papers*, ISSN 1398-6465 R9816.
- 28 Ibsen, L.B., Jakobsen, K.P. (1998). Limit State Equations for Stability and Deformation. *AAU Geotechnical Engineering Papers*, ISSN 1398-6465 R9828.
- 29 Praastrup, U., Ibsen, L.B., Lade P.V. (1999). Presentation of Stress Points in the Customised Octahedral Plane. Published in *Proc. 13th ASCE Engineering Mechanics Division Conference, June 13-16, 1999, Baltimore, USA, 6 pages. AAU Geotechnical Engineering Papers*, ISSN 1398-6465 R9906.
- 30 Praastrup, U., Ibsen, L.B., Lade P.V. (1999). A Generic Stress Surface Introduced in the Customised Octahedral Plane. *Proc. 7th Int. Symp. on Numerical Models in Geomechanics, Graz, Austria, Sept. 1.-3. 1999. Balkema, Rotterdam ISBN 90 5809 095 7*, pp 71-76. *AAU Geotechnical Engineering Papers*, ISSN 1398-6465 R9907.
- 31 Ibsen, L.B., Lade P.V. (1999). Effects of Nonuniform Stresses and Strains on Measured Characteristic States. *Proc. 2nd Int. Symp. Pre-failure Deformation Characteristics of Geomaterials, IS Torino 99, Sept. 26.-29.1999*, pp 897-904. *AAU Geotechnical Engineering Papers*, ISSN 1398-6465 R9908.
- 32 Jakobsen, K.P., Praastrup, U., Ibsen, L.B. (1999). The influence of the stress path on the characteristic stress state. *Proc. 2nd Int. Symp. Pre-failure Deformation Characteristics of Geomaterials, IS Torino 99, Sept. 26.-29.1999*, pp 659-666. *AAU Geotechnical Engineering Papers*, ISSN 1398-6465 R9909.
- 33 Praastrup, U., Jakobsen, K.P., Ibsen, L.B. (1999). Two Theoretically Consistent Methods for Analysing Triaxial Tests. Published in *Computers and Geotechnics, Vol. 25(1999)*, pp. 157-170. *AAU Geotechnical Engineering Papers*, ISSN 1398-6465 R9912.
- 34 Ibsen, L.B. (1999). Cyclic Fatigue Model. *AAU Geotechnical Engineering Papers*, ISSN 1398-6465 R9916.

